

# FINITE ELEMENT MESH REDUCTION GUIDELINES FOR THE INVERSE PROBLEM OF SOURCE LOCALIZATION IN PERIPHERAL NERVES

José Zariffa and Milos R. Popovic

*Institute of Biomaterials and Biomedical Engineering, University of Toronto*

*Edward S. Rogers Sr. Department of Electrical and Computer Engineering, University of Toronto*

*Toronto Rehabilitation Institute, Canada*

## INTRODUCTION

Being able to localize the source of electrical activity within a nerve would improve our ability to map neural pathways and to monitor the activity of specific pathways. If this monitoring could be done in real-time, it could improve the bandwidth of information between a user and a neural prosthesis and thereby allow for finer control of the prosthesis. Nerve cuff electrodes can tell us that there is activity somewhere in the nerve, but techniques to determine the location of that activity are currently limited [7]. Intraneural electrode arrays, on the other hand, can give us information only about a few specific sites. The overall objective of our research is to achieve more precise localization of electrical activity within a nerve than what is possible with existing methods, by approaching the issue as an inverse problem of source localization. Using potential recordings from multiple sites at the periphery of the nerve, obtained from a cuff electrode with a large number of contacts, the problem can be formulated as a modified version of the electroencephalography/magnetoencephalography source localization problem [4,5].

Before recovering the source distribution from the electrode measurements (the inverse problem (IP)), we must first construct a model of the peripheral nerve. This model is used to compute the measurements that would result from a unit source placed at each possible location in the discretized region (a process that is known as solving the forward problem (FP)). This information is gathered into an  $N \times M$  matrix known as the leadfield matrix, where  $N$  is number

of measurements and  $M$  is three times the number of possible source locations (there is one column for each of three orthogonal sources at each location). In this study the FP is solved using finite element (FE) modeling. We attempt to reduce the number of elements in the FE mesh without affecting the quality of the solution in a given region of interest (ROI). By reducing the number of mesh elements, we reduce the computational time needed to solve the IP, and also make that problem better determined.

## BACKGROUND

The relationship between the set of measurements  $\mathbf{v}$ , the leadfield matrix  $\mathbf{L}$ , and the discretized source distribution  $\mathbf{j}$  is given in Equation 1 [5].

$$\mathbf{v} = \mathbf{L}\mathbf{j} + \boldsymbol{\varepsilon} \quad (1)$$

$\boldsymbol{\varepsilon}$  is the additive noise. The goal of the IP is to recover  $\mathbf{j}$  when  $\mathbf{v}$  and  $\mathbf{L}$  are known. Typically  $N$  is much smaller than  $M$ , so the problem is ill-posed and has an infinite number of solutions. To overcome this problem, a common strategy is to solve a minimum-norm least-squares problem that yields the solution that has the smallest norm while still satisfying the measurements. Additional information can be incorporated into the problem by minimizing a weighted version of the solution norm. This minimization problem can be expressed as shown in Equation 2, and its solution is shown in Equation 3 [5].

$$\hat{\mathbf{j}} = \arg \min_{\mathbf{j}} \left\{ \|\mathbf{L}\mathbf{j} - \mathbf{v}\|^2 + \lambda \|\mathbf{H}\mathbf{j}\|^2 \right\} \quad (2)$$

$$\hat{\mathbf{j}} = (\mathbf{H}^T \mathbf{H})^{-1} \mathbf{L}^T [\mathbf{L}(\mathbf{H}^T \mathbf{H})^{-1} \mathbf{L}^T + \lambda \mathbf{I}]^{-1} \mathbf{v} \quad (3)$$

$\mathbf{H}$  is a diagonal matrix whose entries are the weights associated with the minimization of each point in the solution space,  $\lambda$  is a parameter that balances the model fitting and the minimization of the weighted norm, and  $\mathbf{I}$  is the identity matrix. Because the expression for the source distribution estimate contains  $\mathbf{L}$ , it is necessary to obtain this matrix before the IP can be addressed. This FP is solved using numerical methods because the complexity of the region under consideration makes analytical approaches prohibitive. For a region with anisotropic conductivity, such as a peripheral nerve, the FE method is the most appropriate [6] and therefore is used here. Each element in the FE mesh corresponds to one entry in  $\mathbf{j}$  and one column  $\mathbf{L}$ . By reducing the number of mesh elements, these matrices can be made smaller, which will lead to faster computations when solving the IP. Furthermore, assuming  $\mathbf{L}$  is of rank  $N$ , the dimension of the nullspace of  $\mathbf{L}$  is  $M-N$ . The nullspace of  $\mathbf{L}$  contains all the source distributions that cannot be detected. An additional advantage of reducing the number of mesh elements is that the dimension of the nullspace of  $\mathbf{L}$  would be slightly reduced as well.

## STRATEGIES FOR MESH REDUCTION

The simplest way to reduce the number of variables is to make the mesh coarser in the FE model (either uniformly or in certain regions). The disadvantage of this approach is that the coarser mesh will have a detrimental impact on the solution of the FP, making the leadfield matrix less accurate and harming rather than helping our efforts to solve the IP. The alternative approach suggested here is to solve the FP with as fine a mesh as is computationally feasible, and then group certain mesh elements together for the purposes of solving the IP. The leadfield columns for all the elements in a group are averaged together to obtain a single new column, for each of the three source orientations. As a result the number of variables in the IP is reduced without affecting the FP computations. The resulting groups of mesh elements are not proper mesh elements themselves (e.g., not tetrahedral), but it

is a simple matter to map the solution back to the original mesh once an inverse solution has been obtained. The remaining problem is therefore how to choose which mesh elements to group together. We propose two criteria.

The first possible justification for grouping two variables is that they cannot be reliably distinguished by source localization algorithms. Depending on the number and location of the electrode contacts, the nerve properties, and the mesh coarseness, two mesh elements may be indistinguishable. In order to quantify such similarity, we compare the leadfield matrix columns corresponding to those two elements. If the norm of the difference of the two vectors is below a certain threshold, the elements are deemed to be indistinguishable. Given the anisotropy of peripheral nerves, it is possible for elements to be indistinguishable when sources are placed in one orientation but not in another.

The second criteria for grouping mesh elements is to define a ROI, then coarsen the mesh outside of that region by forming groups of adjacent elements (regardless of their distinguishability). The mesh coarseness in the ROI is therefore not affected, while the total number of variables is reduced. In peripheral nerves, the main goal is to identify the pathways that are active, meaning that we are more interested in the radial position of the sources within a cross-section than in their longitudinal position along the nerve. The ROI can therefore be a thin slice of the nerve, whose exact longitudinal location is not of critical importance. The slice need only be thick enough to ensure that it will include nodes of Ranvier for all myelinated axons in the nerve.

## METHODS

A FE model of a 2 cm segment of a single-fascicle rat sciatic nerve was constructed, including the endoneurium, perineurium, and epineurium layers, a cuff electrode around the nerve, saline and connective tissue layers between the nerve and electrode, and a saline bath surrounding the nerve. 10 rings of 13 electrode

contacts were placed in the cuff. Although 130 contacts is more than what is currently available in existing electrodes, the number of contacts per ring is based on existing designs (e.g. [7]), and for the purposes of this simulation study having a large number of contacts is helpful for the evaluation of the methods proposed. The leadfields were computed with the help of the SCIRun environment [1].

Three active myelinated axons were simulated at randomly generated radial positions by placing three sets of twenty dipolar sources (corresponding to nodes of Ranvier), oriented along the axis of the nerve. The ROI was defined as a 2 mm segment halfway up the nerve model, corresponding to layers 61 to 99 of the 159 layers making up the FE model. The density of the layers was greater in the ROI in order to obtain a more precise view of the activity in that area. The ROI contained 5 of the 60 sources. Simulated measurements were obtained using the leadfield derived from the unmodified mesh. No noise was added for the purposes of this study.

To examine the effects of similarity-based groupings, mesh elements were grouped based on their similarity in the longitudinal direction. This criterion is for illustrative purposes only; ideally, two elements should be grouped only if they are indistinguishable in all three orientations. Two leadfield columns were deemed to be similar if the norm of their difference was smaller than 1% of the largest of the two column norms. Groups were defined to contain at most 4 connected elements.

To examine the effects of the ROI-based groupings, mesh elements in layers 1 to 50 and 110 to 159 were grouped into groups of up to 3 connected elements. Note that the groupings are performed using simple algorithms (for both this case and the previous one) that are by no means optimal, but are sufficiently effective for the purposes of this paper.

The IP was solved using the unmodified leadfield and each of the two modified ones. In each case, the method used was the standardized FOCUSS method, run for 200 iterations and initialized with standardized LORETA [2,3], with

no additional regularization. The standardization method was modified to account for the anisotropy (each leadfield column, rather than each mesh element, had a separate normalization factor). The solution space was limited to the endoneurium, which accounts for 20274 of the 85962 elements in the original mesh (excluding the saline bath).

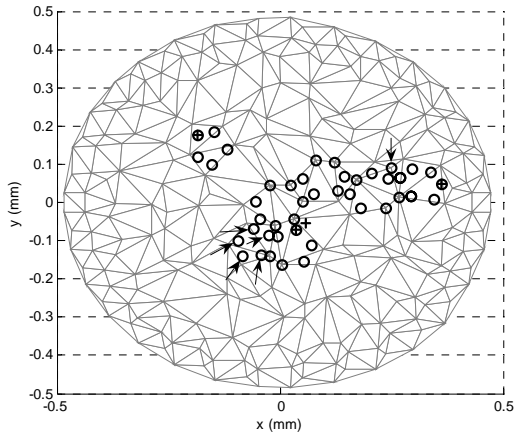
## RESULTS

Table 1 displays the size of the three leadfield matrices, as well as the time required to solve the IP with each leadfield on a 3 GHz Pentium 4 PC.

**Table 1: Effect of groupings on matrix size and IP solution time**

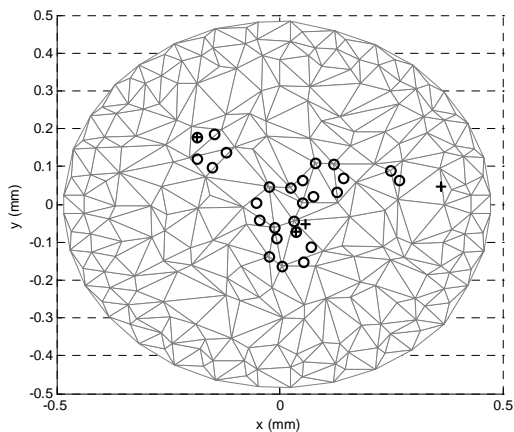
Leadfield	Matrix Size	Time to Solve IP
Unmodified	130x60822	431.95 s.
Similarity-based grouping	130x27213	192.19 s.
ROI-based grouping	130x39549	290.77 s.

Figure 1 shows the solution of the IP using the unmodified leadfield. All the localized sources from the 39 layers in the ROI are projected onto a single cross-section, i.e. each circle represents the radial position of one element of the solution in the ROI, with the height information removed. The figures do not contain any information regarding activity outside the ROI, because our goal was to maintain the quality of the solution in the ROI only. The plus signs indicate the location of the true sources. A perfect solution would therefore consist of having a circle around each plus sign, and nowhere else. Figure 1 shows that although there are spurious elements in the solution, the general pattern gives a reasonable representation of the true sources. The solution using the similarity-based grouping criterion is identical except for the absence of the locations indicated by arrows in the figure. The groupings therefore led to fewer spurious elements, slightly improving the solution.



**Figure 1: Localization with similarity-based groupings**

Figure 2 displays the solution obtained using the ROI-based criterion. It is noticeably sparser and the rightmost axon is not found (i.e. not circled).



**Figure 2: Localization with ROI-based groupings**

If, in addition, we display elements that are indistinguishable from the elements present in Figure 2 for sources in the longitudinal direction, we obtain Figure 3, where all three axons are now localized. This last experiment highlights the fact that distinguishability should be taken into account when interpreting solutions.

## CONCLUSION

Distinguishability of mesh elements is important for the interpretation of the IP solution, and can effectively be used as a grouping criterion. Groupings based on the ROI were less effective but with careful interpretation the

locations of the true sources could still be recovered. Both groupings resulted in faster IP computations. More work in this direction is warranted in order to help speed up IP solutions, which is crucial to eventual real-time implementation and applications to control of neural prostheses.

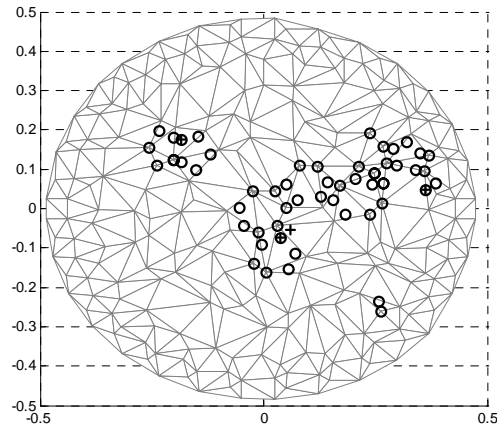


**Figure 3: Solution after addition of locations similar to those shown in Figure 2**

## ACKNOWLEDGEMENTS

This work was supported by the Natural Sciences and Engineering Research Council of Canada.

## REFERENCES

- [1] SCIRun: A Scientific Computing Problem Solving Environment. Scientific Computing and Imaging Institute (SCI), <http://software.sci.utah.edu/scirun.html>, 2002.
- [2] Gorodnitsky I.F., George J.S., and Rao B.D. (1995). "Neuromagnetic source imaging with FOCUSS: a recursive weighted minimum norm algorithm," *Electroencephalogr. Clin. Neurophysiol.*, 95(4):231-251.
- [3] Liu H., Schimpf P.H., Dong G., Gao X., Yang F., and Gao. S. (2005). "Standardized shrinking LORETA-FOCUSS (SSLOFO): a new algorithm for spatio-temporal EEG source reconstruction," *IEEE Trans. Biomed. Eng.*, 52(10):1681-1691.
- [4] Pascual-Marqui, R.D. (1999). "Review of methods for solving the EEG inverse problem," *IJBEM*, 1(1):75-86.
- [5] Phillips C., Mattout J., Rugg M.D., Maquet P., and Friston K.J. (2005). "An empirical Bayesian solution to the source reconstruction problem in EEG," *NeuroImage*, 24(4):997-1011.
- [6] Weinstein D., Zhukov L., and Johnson C. (2000). "Leadfield bases for electroencephalography source imaging," *Ann. Biomed. Eng.*, 28(9):1059-1065.
- [7] Yoo, P.B., and Durand, D.M. (2005). "Selective recording of the canine hypoglossal nerve using a multicontact flat interface nerve electrode," *IEEE Trans. Biomed. Eng.*, 52(8):1461-1469.